Angela Bonaccorso

Istituto Nazionale di Fisica Nucleare
Sezione di Pisa

16th Varenna Conference on Nuclear Reaction Mechanisms

Varenna 12-16 June 2023

Nuclear reaction cross sections and the optical potentials for the n-^{12}C and N-^{12}C scattering

In collaboration with Imane Moumene, INFN-GGI, Firenze,

now at Milano University.

Goal: need accurate S-matrices→ phase shifts→optical potentials in the eikonal approach for a ^{12}C target

Breakup formulae

$$\sigma_{-n}^{inel} = \int d^2\mathbf{b_c}|S_{ct}(\mathbf{b_c})|^2 \int d^2\mathbf{r}_\perp(1-|S_n(\mathbf{b_n})|^2)|\tilde{\phi}_0(\mathbf{r}_\perp)|^2$$

$$\sigma_{-n}^{el} = \int \mathrm{d}^2\mathbf{b}_c|S_{ct}\left(\mathbf{b}_c\right)|^2 \int \mathrm{d}^2\mathbf{r}_\perp\left|1-S_n\left(\mathbf{b}_n\right)\right|^2\left|\tilde{\phi}_0\left(\mathbf{r}_\perp\right)\right|^2.$$

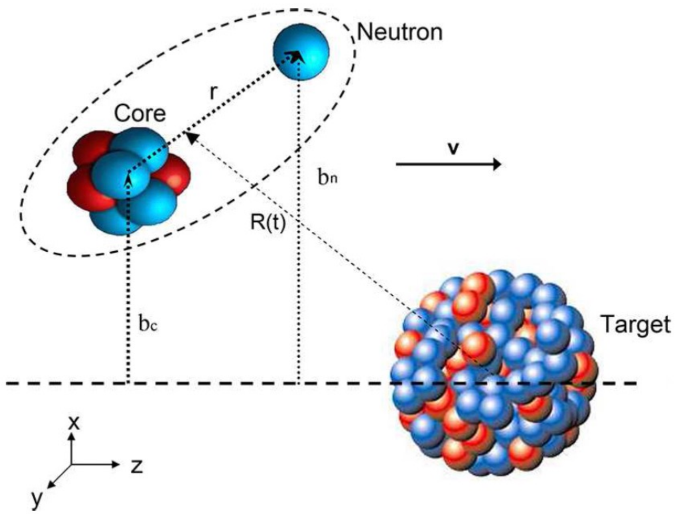

See also *arXiv:2212.06056v2*

C. Hebborn, T. R. Whitehead, A. E. Lovell,3 and F. M. Nunes,

Comparison between phenomenological potentials and single folding and/or double folding potentials

S.F.

$$W^{NN}(\mathbf{r}) = \int d\mathbf{b}_1 W^{nN}(\mathbf{b}_1 - \mathbf{b}, z) \int dz_1 \rho(\mathbf{b}_1, z_1). \qquad (4)$$

D.F.

$$W^{NN}(\mathbf{r}) = -\frac{1}{2}\hbar v \sigma_{nn} \int d\mathbf{b}_1 \rho_p(\mathbf{b}_1 - \mathbf{b}, z) \int dz_1 \rho_t(\mathbf{b}_1, z_1). \qquad (5)$$

Also

s.f.

$$W^{nN}(\mathbf{r}) = -\tfrac{1}{2}\hbar v \sigma_{nn} \rho_t(\mathbf{r}) \qquad (6)$$

Motivations to fit optical potentials

The Optical Potential (OP) is obtained from the reduction of the many body scattering problem to a one body Schrödinger equation

A good OP can give useful information on the structure of a nucleus besides helping describing complex reactions.

- ^{12}C and ^{9}Be are the most used targets for nuclear breakup (knockout) with RIBs
- **Energy dependence of the OP**
- Phenomenological vs *microscopic* OP.
- n+^{9}Be
- n+ ^{12}C
- ^{12}C+^{12}C as a test
- ^{12}C+^{9}Be

More Motivations to calculate reaction cross section

- An immediate test for the accuracy of the imaginary part of the optical potential. Plenty of data to compare to.
- Reaction cross section data are crucial in optical model analyses of elastic scattering, and they can in many cases eliminate ambiguities present in calculations based only on angular distributions.
- Realistic nuclear reaction cross-section (σ_R) models are an essential ingredient of reliable heavy-ion transport codes. Such codes are used for risk evaluation of manned space exploration missions as well as for ion-beam therapy dose calculations and treatment planning.
- From the beginning of physics with RIBs comparison of measured and calculated σ_R has been applied to deduce density distributions of exotic nuclei as well as their root mean square radii (rms). (Tanihata et al., Y. Suzuki et al.…)
- **Predictive power of models**?

PHYSICAL REVIEW C, VOLUME 61, 034605

Final state interaction effects in breakup reactions of halo nuclei

A. Bonaccorso*
Institute for Nuclear Theory, Seattle, Washington 98195-1550
and Istituto Nazionale di Fisica Nucleare, Sezione di Pisa, I-56100 Pisa, Italy†

F. Carstoiu
Institute of Atomic Physics, P.O. Box MG-6, Bucharest, Romania
(Received 1 October 1999; published 11 February 2000)

ELSEVIER

Nuclear Physics A 706 (2002) 322–334

NUCLEAR PHYSICS A

www.elsevier.com/locate/npe

Optical potentials of halo and weakly bound nuclei

A. Bonaccorso [a,*], F. Carstoiu [b]

Few-Body Syst (2016) 57:331–336
DOI 10.1007/s00601-016-1082-4

CrossMark

A. Bonaccorso · F. Carstoiu · R. J. Charity · R. Kumar
G. Salvioni

Differences Between a Single- and a Double-Folding Nucleus-^{9}Be Optical Potential

PHYSICAL REVIEW C **94**, 034604 (2016)

Imaginary part of the ^{9}C -^{9}Be single-folded optical potential

A. Bonaccorso,[1,*] F. Carstoiu,[2] and R. J. Charity[3]

N+N The Glauber reaction cross section is given by

$$\sigma_R = 2\pi \int_0^\infty bdb(1 - |S_{NN}(\mathbf{b})|^2), \qquad (1)$$

where

$$|S_{NN}(\mathbf{b})|^2 = e^{2\chi_I(b)} \qquad (2)$$

is the probability that the nucleus-nucleus (NN) scattering is elastic for a given impact parameter $\mathbf{b}$.

The imaginary part of the eikonal phase shift is given by

$$\chi_I(\mathbf{b}) = \frac{1}{\hbar v}\int dz W^{NN}(\mathbf{b},z)$$
$$= \frac{1}{\hbar v}\int dz \int d\mathbf{r_1} W^{nN}(\mathbf{r_1}-\mathbf{r})\rho(\mathbf{r_1}), \qquad (3)$$

where W^{NN} is negative defined as

S.F.
$$W^{NN}(\mathbf{r}) = \int d\mathbf{b_1} W^{nN}(\mathbf{b_1}-\mathbf{b},z)\int dz_1\rho(\mathbf{b_1},z_1). \qquad (4)$$

D.F.
$$W^{NN}(\mathbf{r}) = -\frac{1}{2}\hbar v\sigma_{nn}\int d\mathbf{b_1}\rho_p(\mathbf{b_1}-\mathbf{b},z)\int dz_1\rho_t(\mathbf{b_1},z_1). \qquad (5)$$

Also

s.f.
$$W^{nN}(\mathbf{r}) = -\tfrac{1}{2}\hbar v\sigma_{nn}\rho_t(\mathbf{r}) \qquad (6)$$

The double folding (5) for $\mathbf{W^{NN}}$ is conceptually **wrong** because the interaction acts only to first order, infact it was originally introduced for the REAL part. Eq.(4) with a phenomenological W^{nN} is in principle more accurate.

First I will discuss the difference between a phenomenological W^{nN} and others obtained by Eq.(6).

Then I will compare results for σ_r with W^{NN} from Eq.(4) with a phenomenological W^{nN} and with W^{NN} from Eq.(5)

As an intermediate step….

PHYSICAL REVIEW C, VOLUME 62, 034608

Scatterings of complex nuclei in the Glauber model

B. Abu-Ibrahim* and Y. Suzuki

$$e^{i\tilde{\chi}_{\mathrm{OLA}}(\boldsymbol{b})} = \exp\left(-\int d\boldsymbol{r}\, \rho_P(\boldsymbol{r}) \Gamma_{NT}(\boldsymbol{\xi}+\boldsymbol{b})\right),$$

Modified Optical Limit **(MOL)**

$$\Gamma_{NT}(\boldsymbol{b}) = \sum_{k=1}^{K} \frac{1-i\alpha_k}{4\pi\beta_k} \sigma_k \exp\left(-\frac{\boldsymbol{b}^2}{2\beta_k}\right),$$

Nucleon-target profile function.
Can be interpreted as the z-integral of a nucleon-target microscopic optical potential

α_{nn}=Re $f_{nn}(0)$/Im $f_{nn}(0)$

Angela Bonaccorso

A.B & R. J. Charity, PRC89, 024619 (2014)

n+^{9}Be

Resonances described by $\delta V(r) = 16\alpha \frac{e^{2(r-R^R)/a^R}}{(1+e^{(r-R^R)/a^R})^4}$. consistent with dispersive contribution

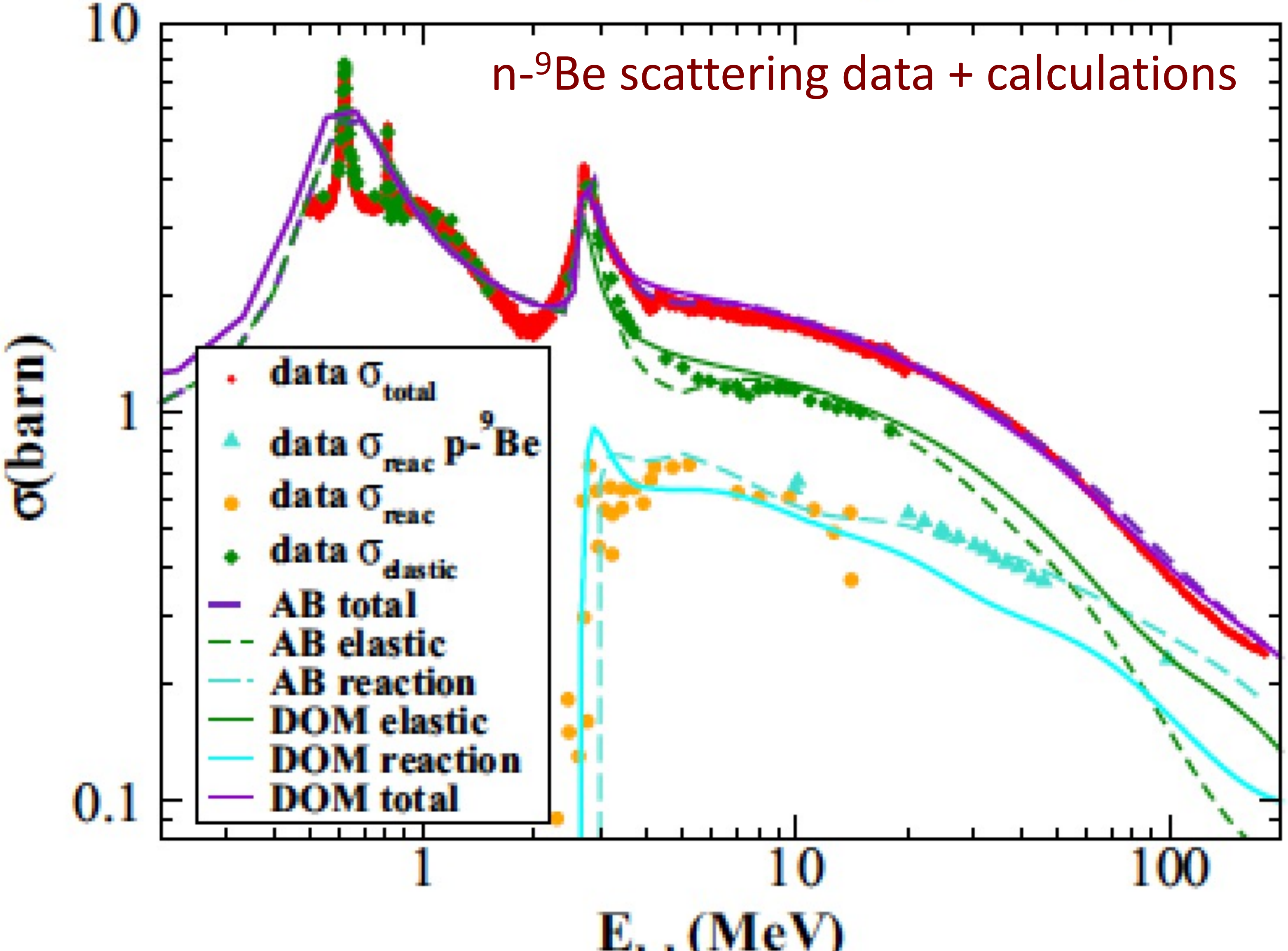

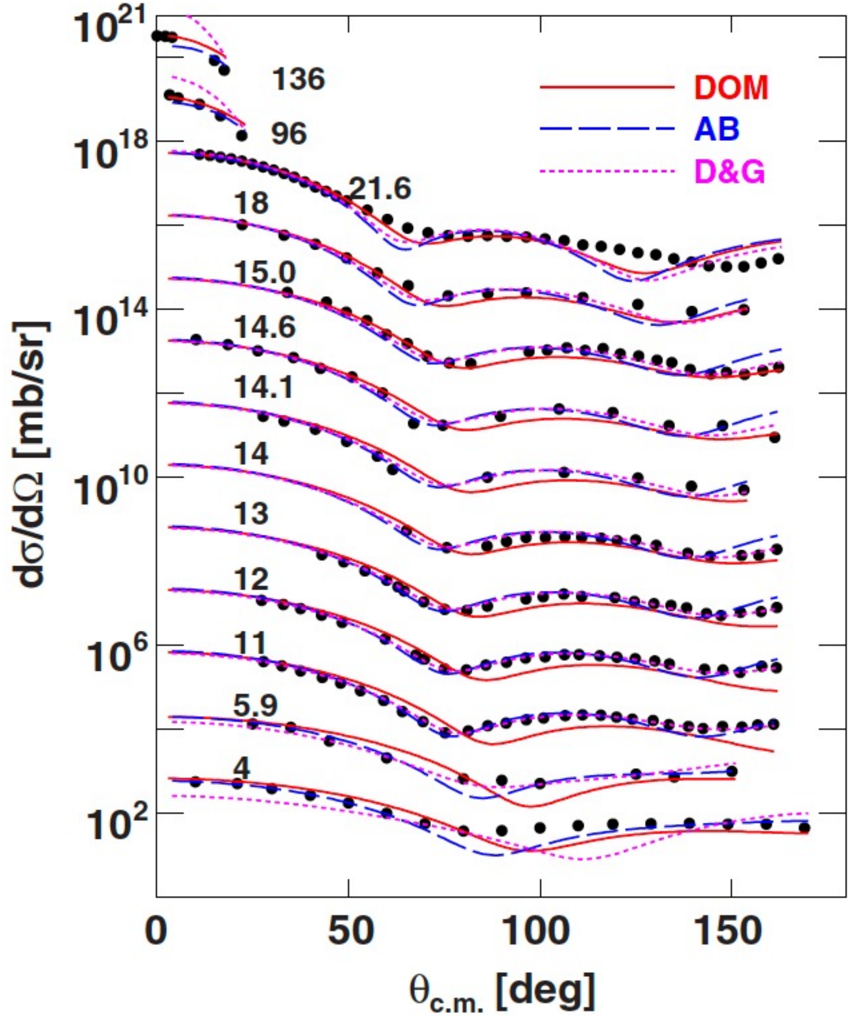

Phenomenological potentials

E_{lab} (MeV)	V^R (MeV)	r_0^R (fm)	a^R (fm)	W^{sur} (MeV)	W^{vol} (MeV)
$20 \leq E_{lab} < 40$	$31.304 - 0.145E_{lab}$	$1.647 - 0.005(E_{lab} - 5)$	$0.3\text{-}0.0001E_{lab}$	$1.65 + 0.365E_{lab}$	$5.6 - 0.005(E_{lab} - 20)$
$40 \leq E_{lab} < 111$	"	"	"	$16.25 - 0.05(E_{lab} - 40)$	$5.5 - 0.01(E_{lab} - 40)$
$111 \leq E_{lab} < 160$	"	"	0.288	12.7	4.8
$160 \leq E_{lab} < 200$	"	"	"	$12.7 - 0.025(E_{lab} - 160)$	$4.8 - 0.025(E_{lab} - 160)$
$200 \leq E_{lab} < 215$	"	"	"	$11.7 + 0.02(E_{lab} - 200)$	$3.8 + 0.02(E_{lab} - 200)$
$215 \leq E_{lab} \leq 500$	0	"	"	"	"

TABLE I: Energy-dependent optical-model parameters for the (AB) potential for n+^{9}Be. r_0^I=1.3 fm, a^I=0.3 fm at all energies.

E_{lab} (MeV)	V^R (MeV)	r_0^R (fm)	a^R (fm)	W^{sur} (MeV)	W^{vol} (MeV)
$160 \leq E_{lab} < 200$	$31.304 - 0.145E_{lab}$	$1.647 - 0.005(E_{lab} - 5)$	0.288	$12.7 - 0.025(E_{lab} - 160)$	$4.8 - 0.025(E_{lab} - 160)$
$200 \leq E_{lab} < 215$	"	"	"	11.7	3.8
$215 \leq E_{lab} < 220$	0	"	"	"	"
$220 \leq E_{lab} \leq 500$	"	0.1	"	$11.7 + 0.02(E_{lab} - 220)$	$3.8 + 0.02(E_{lab} - 220)$

TABLE II: Energy-dependent optical-model parameters of the potential n-^{12}C for $E_{lab} \geq$160MeV. At lower energies, the parametrization is the same as for ^{9}Be on Table I.

Total experimental and calculated cross sections. Lower blue symbols for ^{9}Be, upper red symbols for ^{12}C. The optical model calculations are given by the orange and cyan dashed lines, respectively. The solid green line is a calculation made with a DOM potential obtained for ^{12}C and applied to ^{9}Be. DOM calculations (LHS) curtesy of Mack Atkinson (LLNL)

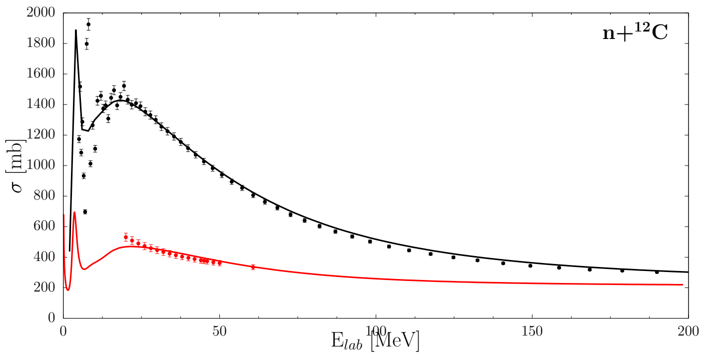

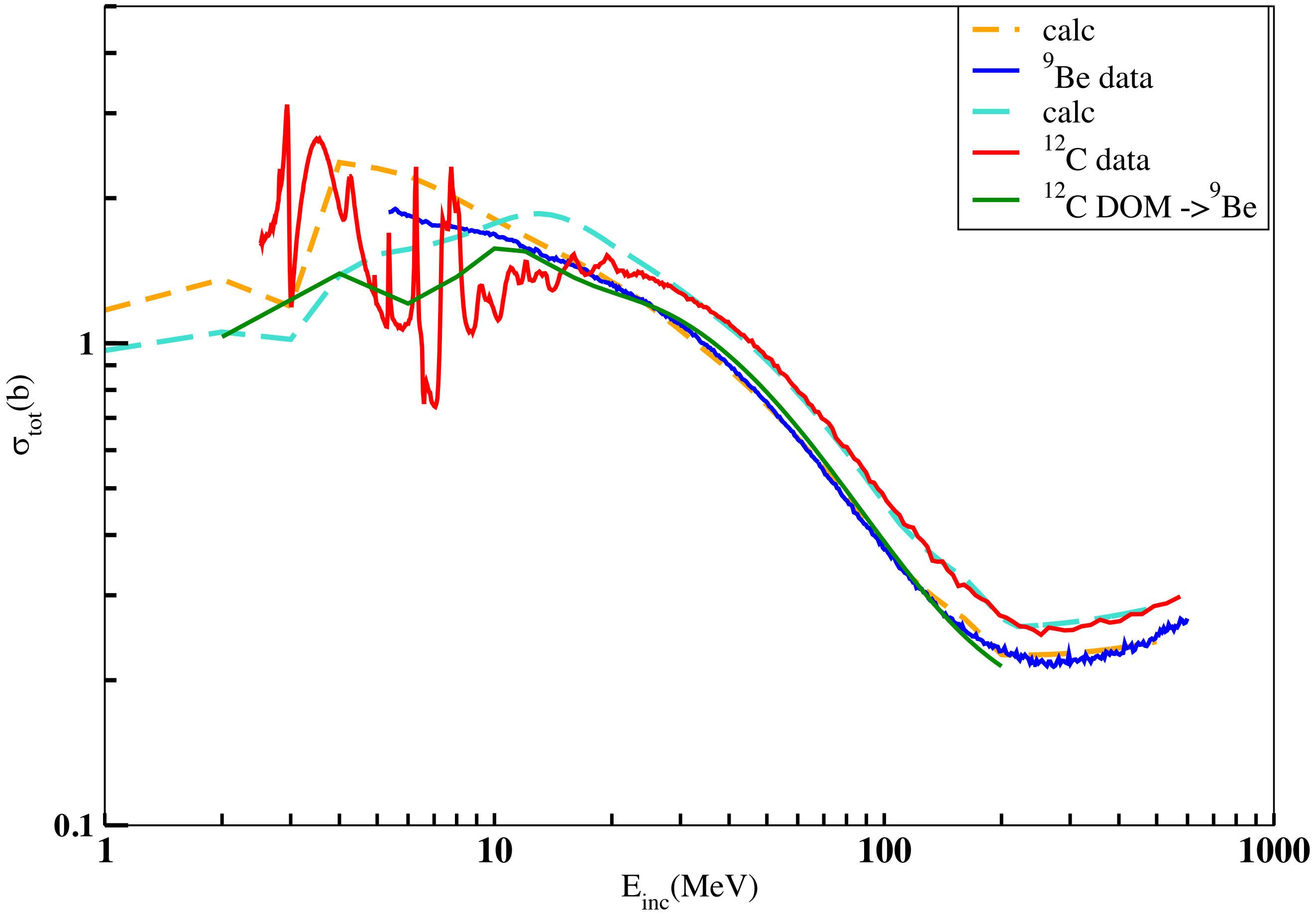

^{12}C

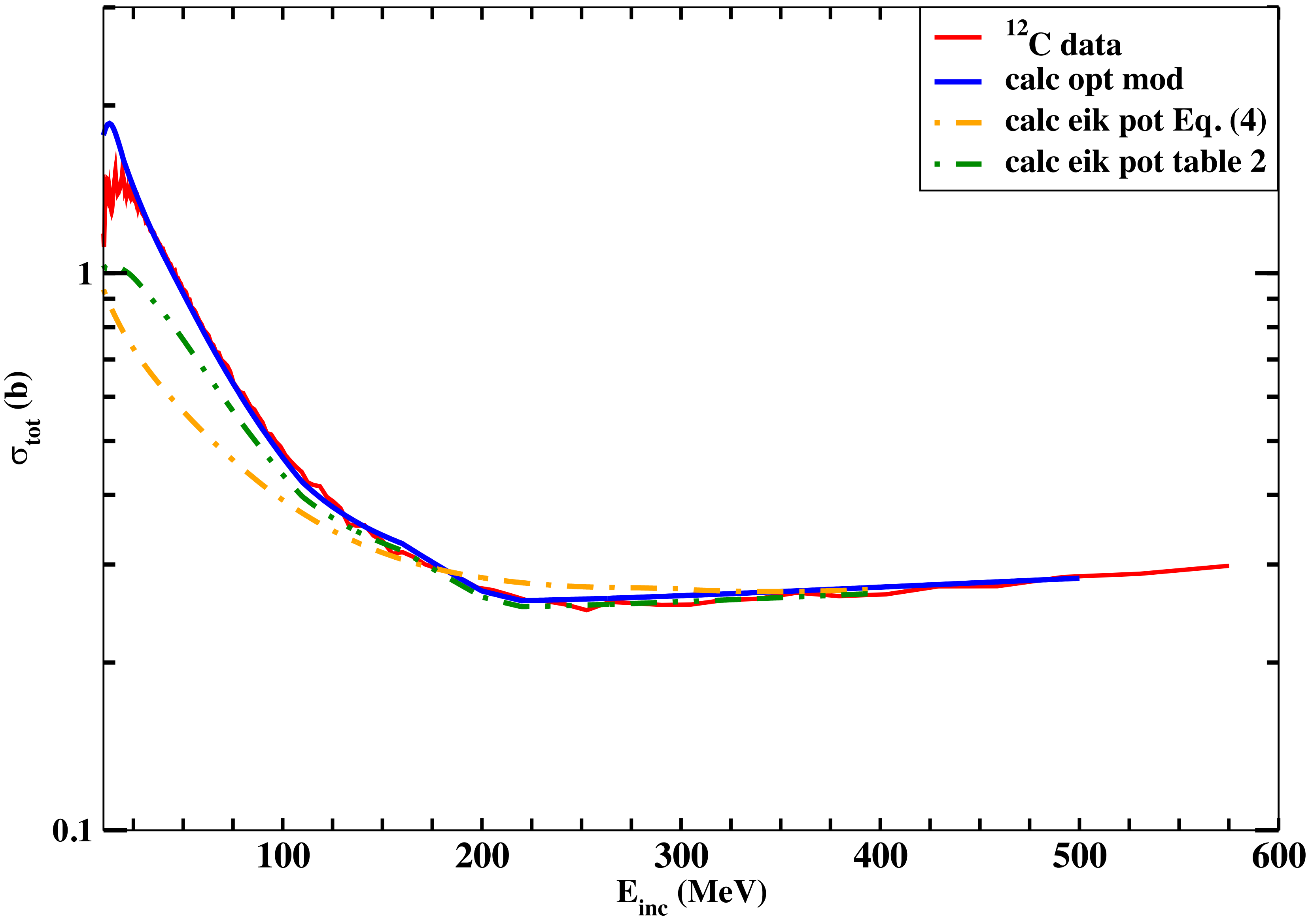

12C data
calc opt mod
calc eik pot Eq. (4)
calc eik pot table 2
σtot (b)
Einc (MeV)
1
0.1
100
200
300
400
500
600

n+ ^{12}C , ^{12}C+ ^{12}C

We confirm dominance of surface absorption for light systems A. Ingemarsson and M. Lantz
Phys. Rev. C 67, 064605

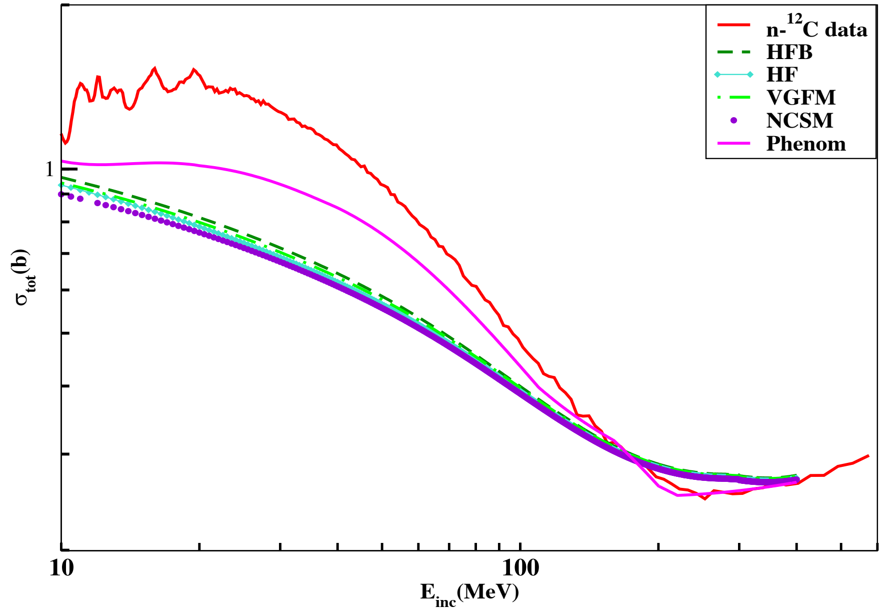

$$W^{nN}(\mathbf{r}) = -\tfrac{1}{2}\hbar v \sigma_{nn} \rho_t(\mathbf{r}) \qquad (6)$$

In medium effects?

Microscopic calculation of in-medium proton-proton cross sections

G. Q. Li and R. Machleidt

Phys. Rev. C 49, 566

σ_nn can be fixed but what about α_nn ?

MOL: B. Abu-Ibrahim and Y. Suzuki, Phys. Rev. C 62, 034608 (2000).

VGFM(Wiringa) NV2+3-IIb*
https://www.phy.anl.gov/theory/research/density/
Light-Nuclei Spectra from Chiral Dynamics
M. Piarulli et al., Phys. Rev. Lett. 120, 052503

NCSM M. Vorabbi, et al., Phys. Rev. C103, 024604 (2021).

Thanks to Petr Navratil and Michael Gennari
for providing the numerical densities

Also see Phys. Rev. C 99, 044603 (2019)
M. Burrows , Ch. Elster *et al.,*

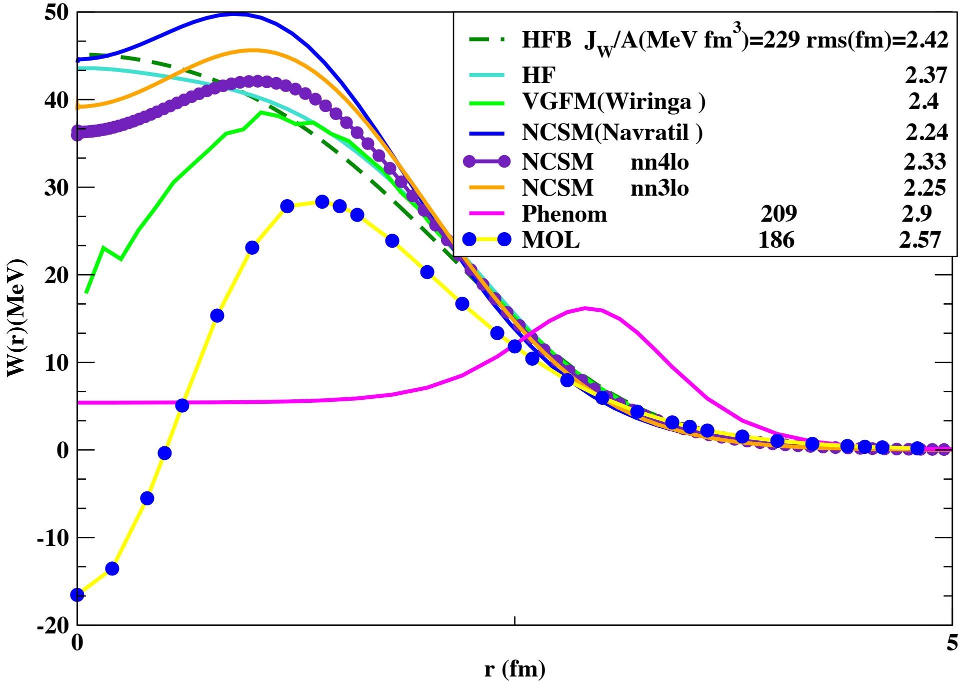

α_{nn}=Re $f_{nn}(0)$/Im $f_{nn}(0)$

- Accurate Re $f_{nn}(0)$ are difficult to obtain and so are the α_{nn}
- There are many papers in the literature offering tables of σ_{nn} and α_{nn} but when used to calculate the energy dependence of n-N elastic xsecs the results are unsatisfactory

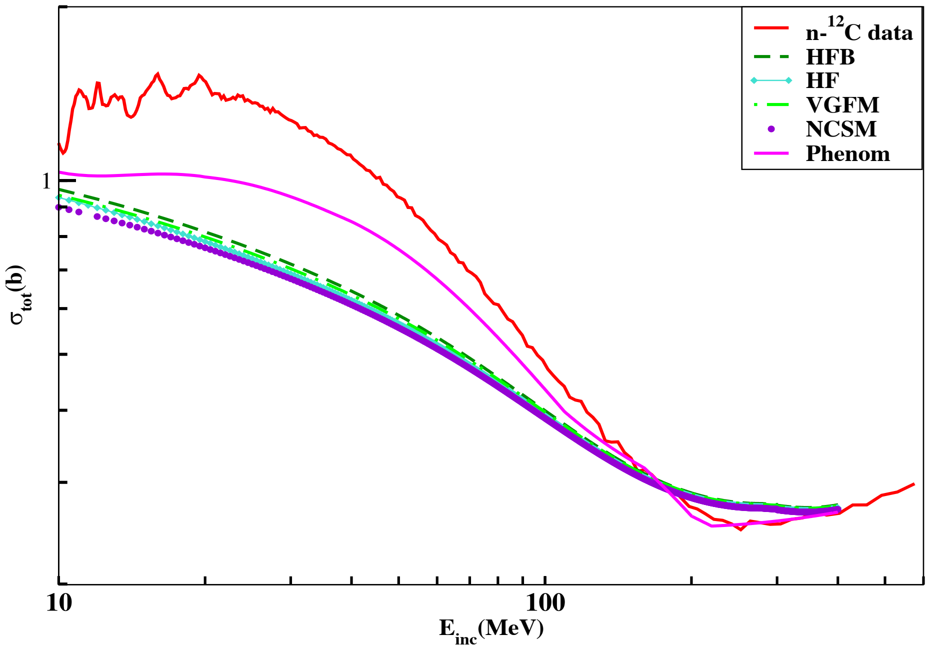

Constant values of α_{nn}

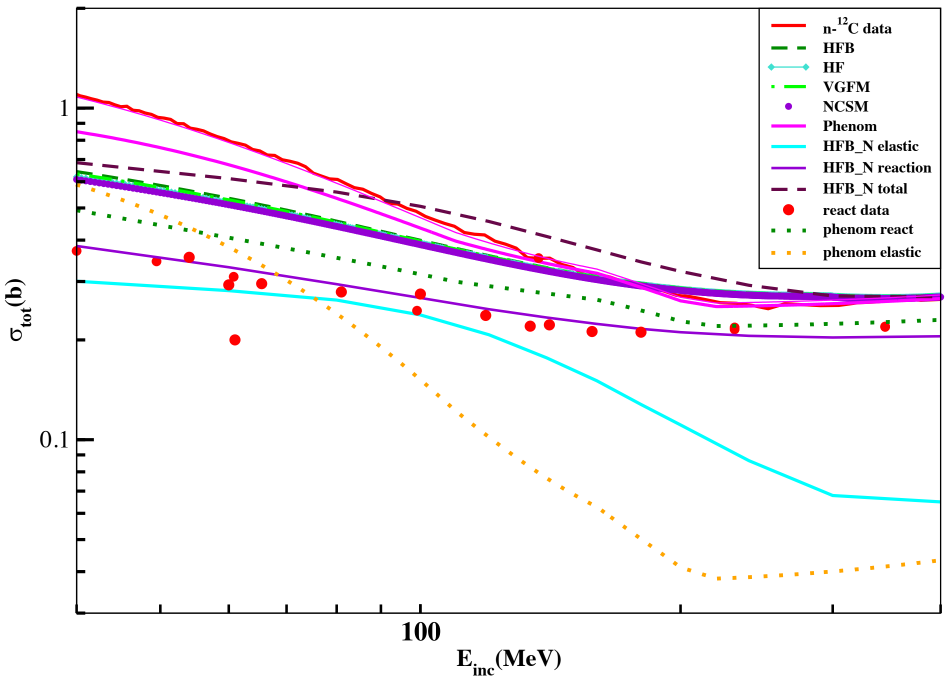

Values of σ_{nn} α_{nn} from B. Abu-Ibrahim et al., Phys. Rev. C 77 (2008) 034607.
They reproduce σ_R but not σ_{tot}

Problem with the absolute values ot total n, p+^{12}C

σ_{el} (J. Klug et a., PRC *68, 064605 (2003),* Elastic neutron scattering at 96MeV from ^{12}C and ^{208}Pb)

- *For 12C, on the other hand, significant differences have been demonstrated between predictions and experiment. Possible explanations might be that ^{12}C exhibits* ***surface effects*** *and deformations coming from a three cluster structure. Another effect, such* ***as a more diffuse edge than anticipated,*** *may also play a role. These contributions have not been taken into account in the model calculations presented here, and therefore it is not surprising that the description of the ^{12}C data is poor in the 30° –50° range. This defectiveness is also found in the evaluated (ENDF-6) cross section, which might call for a reevaluation in the future.*

D.F. vs S.F. for NN potentials

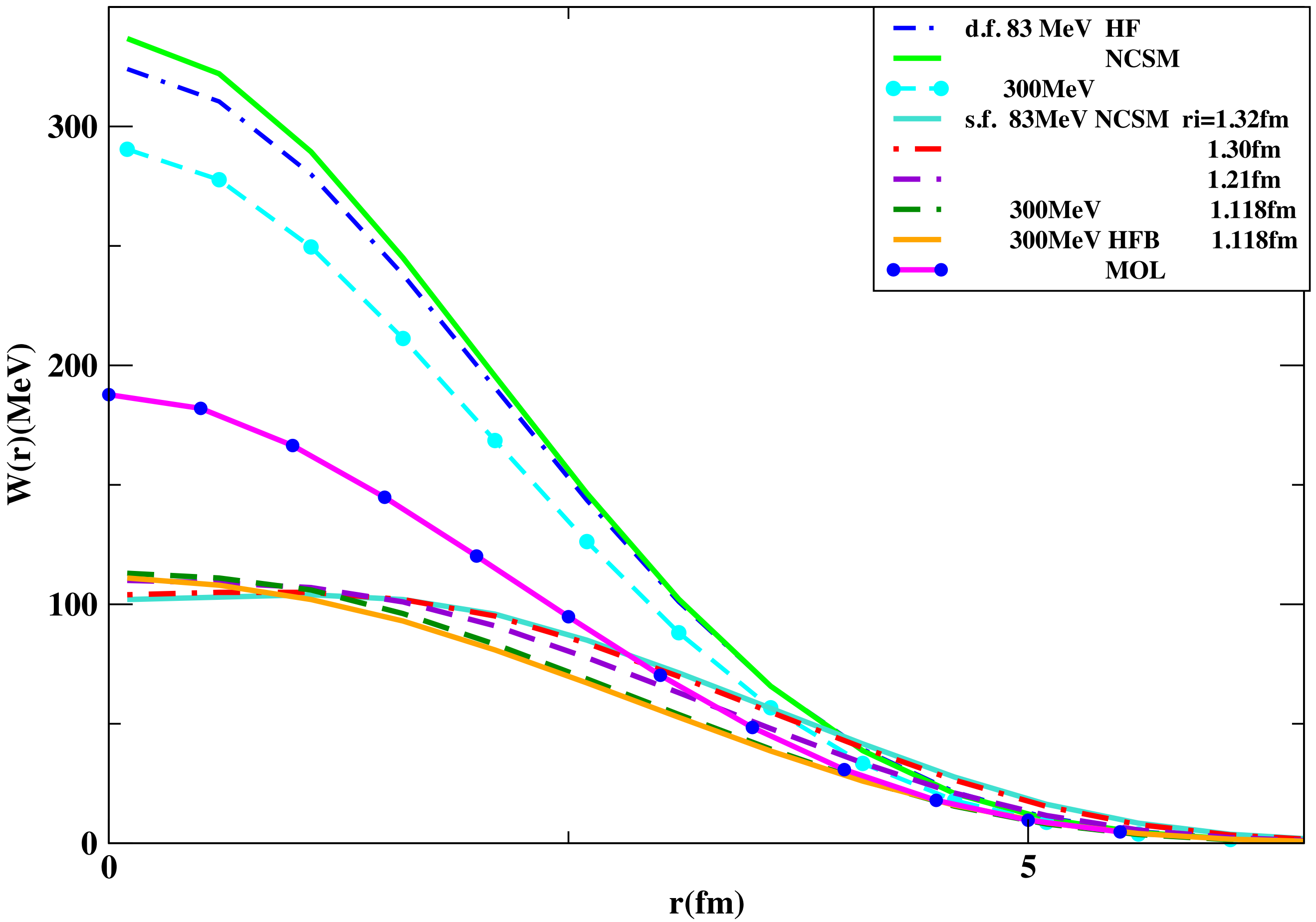

PHYSICAL REVIEW C **79**, 061601(R) (2009)

Reaction cross sections at intermediate energies and Fermi-motion effect

M. Takechi,[1,*] M. Fukuda,[1] M. Mihara,[1] K. Tanaka,[2] T. Chinda,[1] T. Matsumasa,[1] M. Nishimoto,[1] R. Matsumiya,[1] Y. Nakashima,[1] H. Matsubara,[1] K. Matsuta,[1] T. Minamisono,[3] T. Ohtsubo,[4] T. Izumikawa,[5] S. Momota,[6] T. Suzuki,[7] T. Yamaguchi,[7] R. Koyama,[4] W. Shinozaki,[4] M. Takahashi,[4] A. Takizawa,[4] T. Matsuyama,[4] S. Nakajima,[7] K. Kobayashi, M. Hosoi,[7] T. Suda,[2] M. Sasaki,[8] S. Sato,[9] M. Kanazawa,[9] and A. Kitagawa[9]

MOL approch with no simple physical interpretation

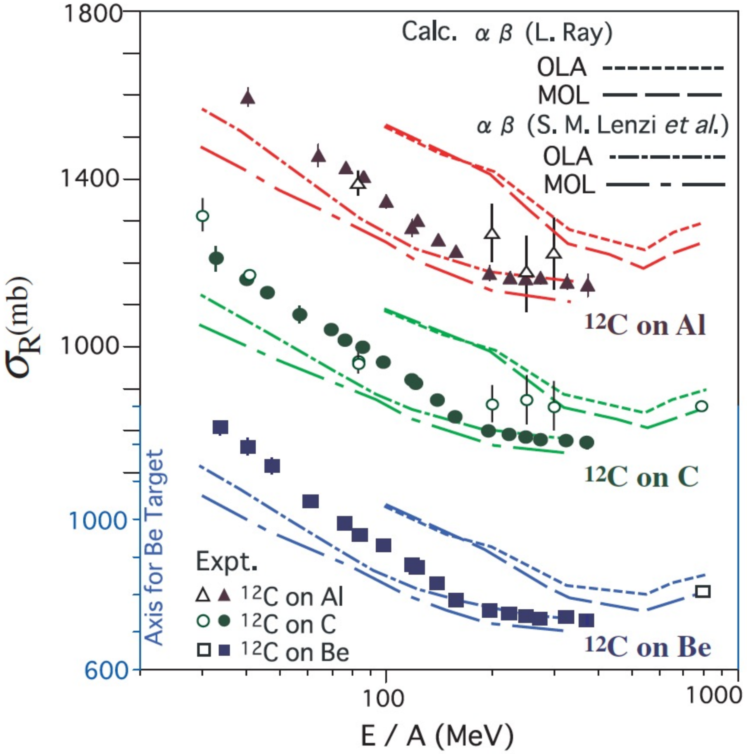

FIG. 1. (Color online) The σ_R data for ^{12}C as a function of beam energy. The closed symbols denote the present data and open symbols denote data from Refs. [8,25–27]. The OLA and MOL calculations were performed using the NN parameters from Ref. [22] (short and long dashed curves) and Ref. [23] (short and long dash-dotted curves).

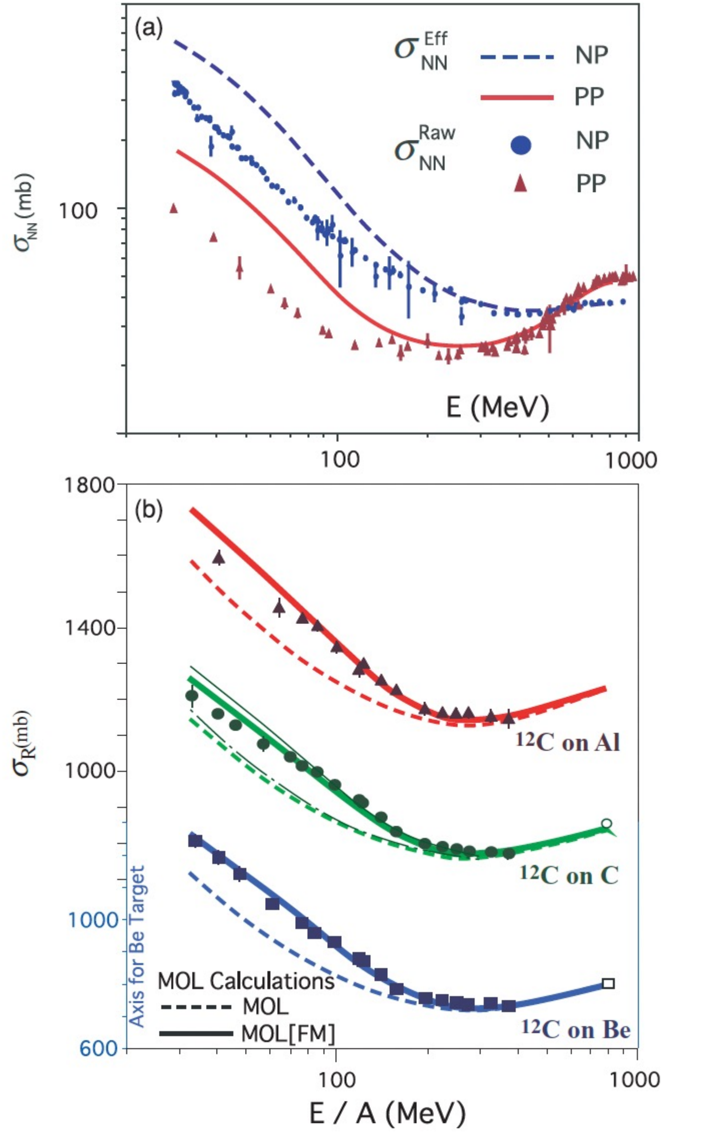

FIG. 2. (Color online) (a) Modified σ_{NN} as effective NN cross section (σ_{NN}^{eff}), which is compared with the raw σ_{NN}. (b) MOL calculations with $\beta(E)$ from Eq. (4) (dashed curve) and MOL[FM] calculations (solid curve) are compared with experimental data. We also show the MOL and MOL[FM] calculations using a Gaussian-type density for the C target (thin solid and dot-dashed curves).

Data from Takechi et al. cf previus slide, Kox

In d.f. $\sigma_{np,pp}$ from De Conti&Bertulani PRC81.064603 (2010).

E_{lab} (MeV)	$r_i(^9Be)$ (fm)	$r_i(^{12}C)$ (fm)
$30\leq E_{lab} \leq 160$	$1.4 - 0.0015E_{lab}$	$1.32 - 0.0013E_{lab}$
$E_{lab} > 160$	1.15	1.118

TABLE III: Energy-dependent optical-model parameter r_i for the (AB) potential for n+^{9}Be and n+^{12}C

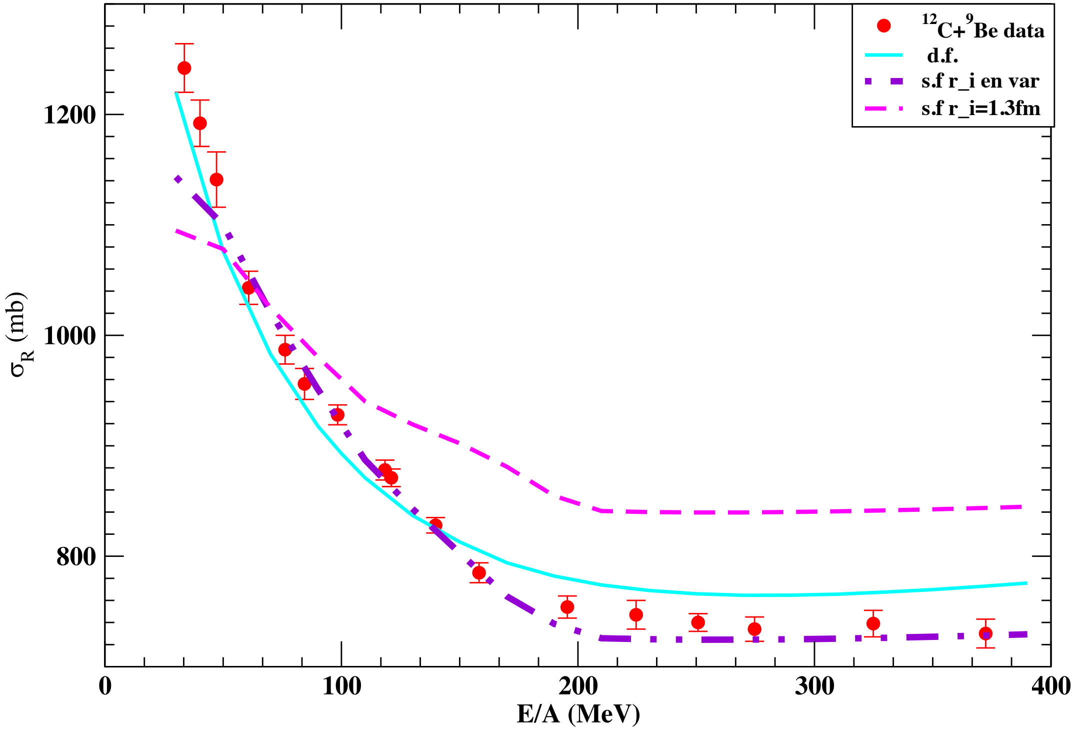

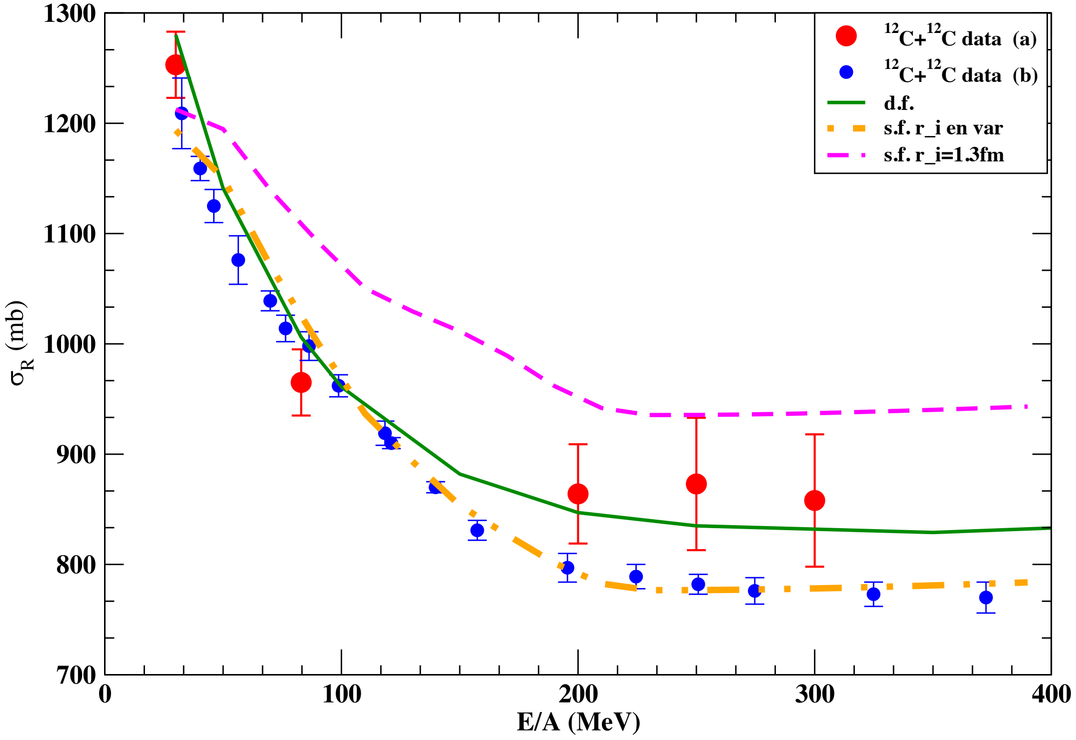

$^{12}C+^{12}C$

E_{inc} (MeV)	model	r_s (fm)	J_W/A_PA_T (MeVfm^3)	r.m.s (fm)	σ_{NCSM} (mb)	r.m.s (mb)	σ_{HF} (mb)	r.m.s	σ_{HFB}
83	S.F.	1.2	184	3.72	994	3.75	1008	3.78	1025
	D.F.	1.22	279	3.29	957	3.36	995	3.43	1027
300	S.F.	1.18	151	3.57	760	3.60	768	3.64	780
	D.F.	1.11	241	3.29	791	3.36	815	3.43	842

280A.MeV

^{12} Ne+^{12}C

E_{inc}(MeV)	model	r_s(fm)	σ_{theo} (mb)	σ_{exp} (mb)
30	S.F.	(1.35) 1.33	(1478) 1456	1550 ±75
	D.F.	1.37	1560	
100	S.F.	(1.27) 1.23	(1327)1211	1161 ± 80
	D.F.	1.21	1206	
200	S.F.	(1.21)1.11	(1193) 1012	1123 ± 80
	D.F.	1.15	1079	
300	S.F.	(1.21)1.12	(1181)1001	1168 ± 100
	D.F.	1.13	1062	

Nucleus	model	r_s(fm]	σ_{theo} (mb)	σ_{exp} (mb)	$r.m.s.$(fm
^{42}Ca	S.F.	(1.23)1.14	(1598) 1388	1463(13)(6)	3.38
	D.F.	1.16	1460		
^{43}Ca	S.F.	(1.22)1.14	(1614)1402	1476(11)(6)	3.40
	D.F.	1.17	1476		
^{44}Ca	S.F.	(1.23)1.15	(1630) 1417	1503(12)(6)	3.42
	D.F.	1.16	1490		
^{46}Ca	S.F.	(1.24)1.15	(1683)1466	1505(8)(6)	3.50
	D.F.	1.17	1543		
^{48}Ca	S.F.	(1.23)1.16	(1714)1495	1498(17)(6)	3.50
	D.F.	1.18	1573		

Conclusions

- We have derived excellent n+^{9}Be, n+^{12}C phenomenological optical potentials up to 500MeV, cross checked vs DOM.
- Excellent single folding P (Core)-T OP validated for ^{12}C + ^{12}C , ^{12}C+^{9}Be. Small volume integrals, large rms radii.
- Dominance of surface absorption (r_i decreases with energy).
- S.F. less ambigous than D.F. (needs to fix a smaller n of parameters)…
- In particular σ_{el} (E_{inc}) for n+^{12}C *not known* and α_{nn}=Re $f_{nn}(0)$/Im $f_{nn}(0)$ for free nn collisions and in medium *not well determined*.
- Evolution of D.F. via nN *ab-initio?*

M. Fukuda et al., private communication; D. Nishimura et al.,Osaka University Laboratory of Nuclear Studies (OULNS) Annual Report 2006, p. 37.

$E_{\rm lab}$ (MeV/nucleon)	$\sigma_{\rm exp}$ (mb)	$\sigma^{\rm VMC}_{\rm d.fold}$ (mb)	$\sigma^{\rm HF}_{\rm d.fold}$ (mb)	$\sigma_{\rm s.fold}$ (mb)	$\sigma^{\rm +surf}_{\rm s.fold}$ (mb)	$\sigma^{\rm bare}_{\rm JLM}$ (mb)	$\sigma^{\rm ren}_{\rm JLM}$ (mb)	$N_{\rm JLM}$	$W_{\rm surf}$ (MeV)	R_s (fm)	$R_s^{\rm fit}$ (fm)	$a^{\rm fit}$ (fm)	r_s (fm)
20		1267	1409	1078	1565	1338	1538	1.65	0.8	6.12	6.25	1.01	1.47
38		1086	1191	1112	1341	1250	1324	1.20	0.5	5.95	5.99	0.97	1.44
40.9	1216 ± 57	1064	1166	1117	1291	1235	1215	0.95	0.4	5.95	5.99	0.98	1.44
43		1050	1148	1103	1275	1221	1260	1.10	0.4	5.95	5.99	0.99	1.44
43.6	1269 ± 22	1046	1144	1106	1235	1219	1257	1.10	0.3	5.82	5.70	0.80	1.40
59		960	1042	1047	1124	1130	1111	0.95	0.2	5.70	5.64	0.82	1.36
61.1	1104 ± 20	950	1030	1045	1122	1119	1119	1.00	0.2	5.68	5.63	0.83	1.36
66		928	1006	1028	1066	1091	1028	0.85	0.1	5.60	5.55	0.80	1.35
67.4	1074 ± 32	923	999	1026	1056	1087	1087	1.00	0.08	5.60	5.53	0.80	1.35
68.3	1064 ± 16	919	995	1024	1052	1082	1063	0.95	0.075	5.55	5.49	0.80	1.33
83		867	934	948	979	1015	987	0.93	0.015	5.40	5.38	0.78	1.29
84.9	981 ± 15	861	928	979	983	1008	989	0.95	0.01	5.40	5.36	0.80	1.29
95		833	895	949	952	968	956	0.97	0.01	5.40	5.28	0.79	1.29
97.2	919 ± 24	827	888	949	951	963	923	0.90	0.005	5.35	5.28	0.80	1.28

Comparison with data, at low energy suggests the need to include the ^{9}C breakup channel explicitly

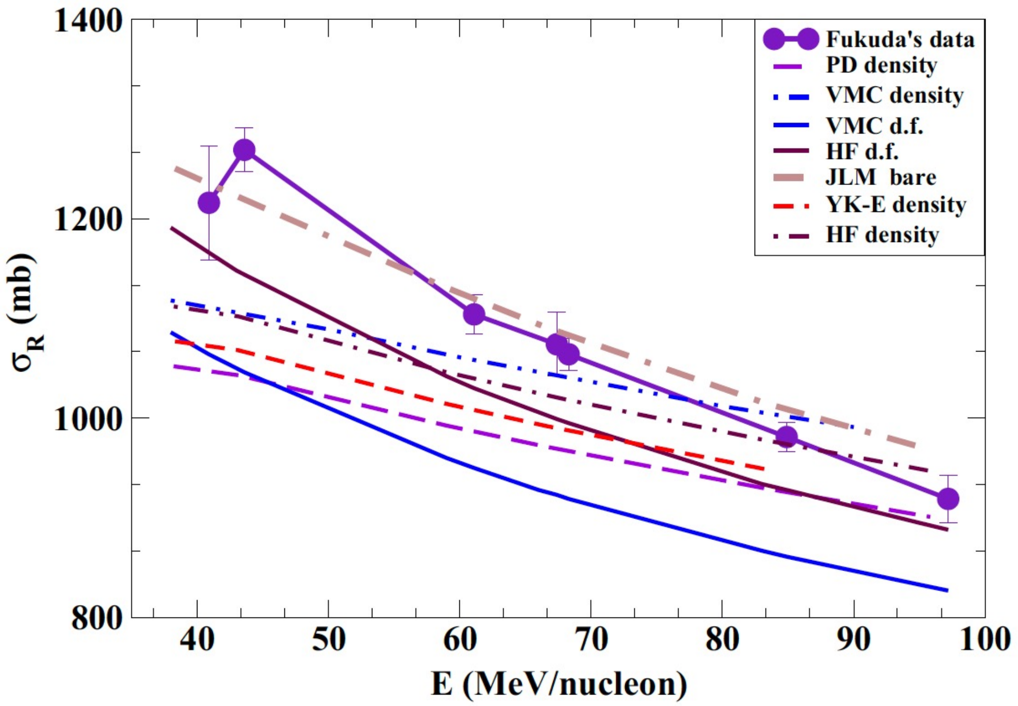

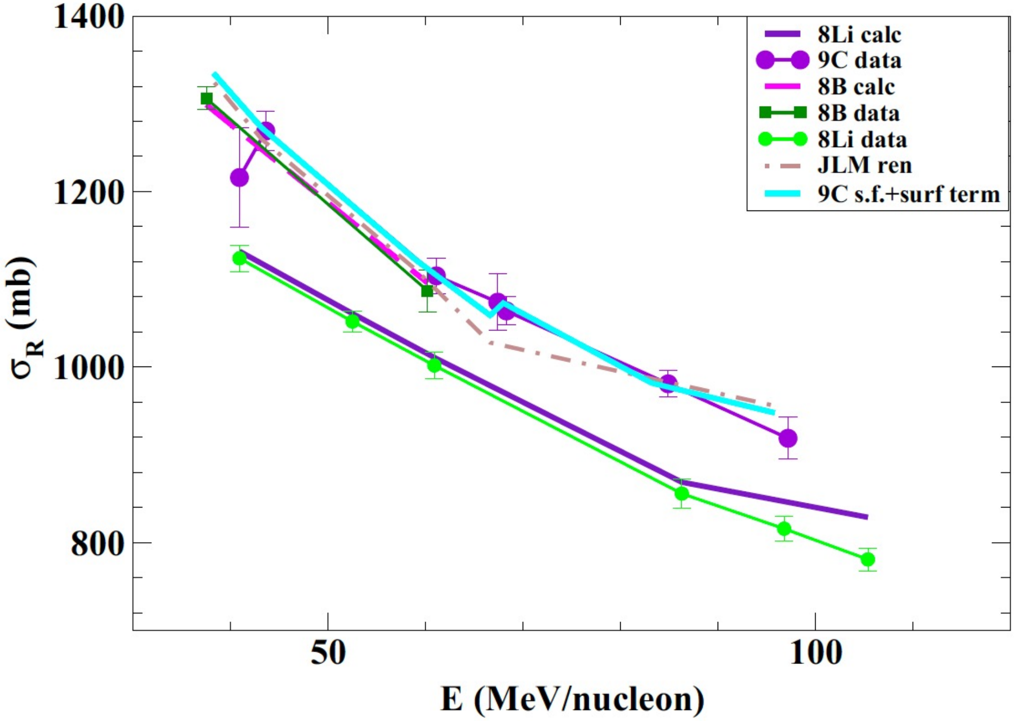

- The above definition of the profile function is equivalent to define a 3d imaginary potential of gaussian shape normalized to 1 whose depth is $-\frac{1}{2}\hbar v\sigma_{nn}$